Structure and Wettability of Methoxy-Terminated Self-Assembled Monolayers on Gold

Irmgard Wenzl, Chi Ming Yam, David Barriet, and T. Randall Lee*

Department of Chemistry, University of Houston, Houston, Texas 77204-5003

Received July 8, 2003. In Final Form: September 17, 2003

This manuscript describes the structure and wettability of self-assembled monolayers (SAMs) derived from the adsorption of a series of ω-methoxyalkanethiols ($CH_3O(CH_2)_nSH$, where $n = 9-14$) onto the surface of gold. Using ellipsometry, polarization modulation infrared reflection absorption spectroscopy (PM-IRRAS), and contact angle measurements, the interfacial properties were examined as a function of chain length. Analysis by ellipsometry revealed a progressive increase in the thickness of the films as the chain length of the adsorbate was increased. Similarly, analysis by PM-IRRAS revealed a progressive increase in the conformational order of the methylene chains of the films. Moreover, the frequency and intensity of two characteristic C−H stretching bands of the methoxy groups were observed to vary systematically as a function of odd- versus even-numbered chain length, reflecting an alternating structural change in the films (i.e., an "odd−even" effect). Studies of contact angle wettability revealed that the methoxy-terminated SAMs were more wettable than SAMs derived from the corresponding methyl-terminated alkanethiols ($CH_3(CH_2)_{n+1}SH$), consistent with a substantial polar influence of the terminal ether moiety. In addition, the contact angles were observed to increase with increasing chain length of the methoxy-terminated SAMs. Moreover, small but systematic variations in wettability as a function of odd- versus even-numbered chain length were also observed; their origin was attributed to the influence of surface dipoles.

Introduction

For several decades, researchers have sought to gain a comprehensive understanding of the forces that govern the wettability of solid surfaces.[1−7] Interfacial wettabilities, which are macroscopically observable phenomena, are known to depend strongly on the relative magnitudes of the solid−liquid interfacial forces, which are themselves dictated by the nanoscale structure and composition of both the contacting liquid and the underlying surface.[8−10] Over the past several years, self-assembled monolayers (SAMs) have served as useful tools for examining the relationships between interfacial wettability and chemical structure/composition. SAMs have found favor among interfacial scientists largely because of their well-defined structures and chemical tunability.[11−13] For example, the most widely studied SAM system—the adsorption of normal alkanethiols onto the surface of gold—is characterized by well-packed highly ordered monolayer films that expose CH_3 groups at the interface.[14−16]

Many studies have examined the effects of substituting the CH_3 groups in these SAMs with a variety of alternative functional groups.[17−22] In particular, our studies have focused on a series of SAMs possessing terminally fluorinated end groups.[23−29] While most of the fluorinated SAMs and related Langmuir−Blodgett (LB) films described in the literature[30−33] exhibit surfaces that are less wettable than related CH_3-terminated films toward a variety of polar and nonpolar contacting liquids, we found

* To whom correspondence should be addressed. E-mail: trlee@uh.edu.

(1) Ellison, A. H.; Fox, H. W.; Zisman, W. A. *J. Phys. Chem.* **1953**, *57*, 622.
(2) Zisman, W. A. *Adv. Chem. Ser.* **1964**, *No. 43*, 1.
(3) Schonhorn, H.; Ryan, F. W. *J. Phys. Chem.* **1966**, *70*, 3811.
(4) Schrader, M. E. *J. Phys. Chem.* **1970**, *74*, 2313.
(5) *Contact Angles, Wettability, and Adhesion*; Fowkes, F. M., Ed.; Advances in Chemistry Series 43; American Chemical Society: Washington, DC, 1964.
(6) Bowden, F. P.; Tabor, D. *The Friction and Lubrication of Solids, Part II*; Oxford University: London, 1969.
(7) Ulman, A. *An Introduction to Ultrathin Films from Langmuir−Blodgett to Self-Assembly*; Academic: New York, 1991.
(8) Wasserman, S. R.; Tao, Y.-T.; Whitesides, G. M. *Langmuir* **1989**, *5*, 1074.
(9) Bain, C. D.; Whitesides, G. M. *J. Am. Chem. Soc.* **1989**, *111*, 7155.
(10) Bain, C. D.; Whitesides, G. M. *J. Am. Chem. Soc.* **1989**, *111*, 7164.
(11) Swalen, J. D.; Allara, D. L.; Andrade, J. D.; Chandross, E. A.; Garoff, S.; Israelachvili, I.; McCarthy, T. J.; Murray, R.; Pease, R. F.; Rabolt, J. F.; Wynne, K. J.; Yu, H. *Langmuir* **1987**, *3*, 392.
(12) Holmes-Farley, S. R.; Reamey, R. H.; Nuzzo, R. G.; McCarthy, T. J.; Whitesides, G. M. *Langmuir* **1987**, *3*, 799.
(13) Troughton, E. B.; Bain, C. D.; Whitesides, G. M.; Nuzzo, R. G.; Allara, D. L.; Porter, M. D. *Langmuir* **1988**, *4*, 365.
(14) Bain, C. D.; Whitesides, G. M. *Angew. Chem., Int. Ed. Engl.* **1989**, *101*, 522.
(15) Dubois, L. H.; Nuzzo, R. G. *Annu. Rev. Phys. Chem.* **1992**, *43*, 437.
(16) Ulman, A. *Chem. Rev.* **1996**, *96*, 1533.
(17) Sagiv, J. *J. Am. Chem. Soc.* **1980**, *102*, 92.
(18) Bain, C. D.; Troughton, E. B.; Tao, Y.-T.; Evall, J.; Whitesides, G. M.; Nuzzo, R. G. *J. Am. Chem. Soc.* **1989**, *111*, 321.
(19) Nuzzo, R. G.; Dubois, L. H.; Allara, D. L. *J. Am. Chem. Soc.* **1990**, *112*, 558.
(20) Bilewicz, R.; Majda, M. *J. Am. Chem. Soc.* **1991**, *113*, 5464.
(21) Laibinis, P. E.; Whitesides, G. M. *J. Am. Chem. Soc.* **1992**, *114*, 1990.
(22) Chailapakul, O.; Crooks, R. M. *Langmuir* **1993**, *9*, 884.
(23) Kim, H. I.; Koini, T.; Lee, T. R.; Perry, S. S. *Langmuir* **1997**, *13*, 7192.
(24) Miura, Y. F.; Takenaga, M.; Koini, T.; Graupe, M.; Garg, N.; Graham, R. L., Jr.; Lee, T. R. *Langmuir* **1998**, *14*, 5821.
(25) Kim, H. I.; Graupe, M.; Oloba, O.; Koini, T.; Imaduddin, S.; Lee, T. R.; Perry, S. S. *Langmuir* **1999**, *15*, 3179.
(26) Graupe, M.; Takenaga, M.; Koini, T.; Colorado, R., Jr.; Lee, T. R. *J. Am. Chem. Soc.* **1999**, *121*, 3222.
(27) Colorado, R., Jr.; Graupe, M.; Takenaga, M.; Koini, T.; Lee, T. R. *Mater. Res. Soc. Symp. Proc.* **1999**, *546*, 237.
(28) Colorado, R., Jr.; Graupe, M.; Kim, H. I.; Takenaga, M.; Oloba, O.; Lee, S.; Perry, S. S.; Lee, T. R. *ACS Symp. Ser.* **2001**, *781*, 58.
(29) Colorado, R., Jr.; Graupe, M.; Shmakova, O. E.; Villazana, R. J.; Lee, T. R. *ACS Symp. Ser.* **2001**, *781*, 276.
(30) Tournilhac, F. G.; Bosio, L.; Bourgoin, J. P.; Vandevyver, M. *J. Phys. Chem.* **1994**, *98*, 4870.
(31) Li, X.-D.; Aoki, A.; Miyashita, T. *Langmuir* **1996**, *12*, 5444.
(32) Mingotaud, C.; Agricole, B.; Nozdryn, T.; Cousseau, J.; Gorgues, A.; Delhaes, P. *Thin Solid Films* **1997**, *300*, 228.
(33) Ohnishi, S.; Ishida, T.; Yaminsky, V. V.; Christenson, H. K. *Langmuir* **2000**, *16*, 2722.

10.1021/la035227x CCC: $25.00
Published on Web 10/29/2003

that substitution of the terminal CH_3 groups with terminal CF_3 groups affords films with enhanced wettabilities toward polar liquids such as water, formamide, acetonitrile, and dimethyl formamide. Moreover, we found that SAMs generated from CF_3-terminated thiols having an even number of carbon atoms were noticeably more wettable than those generated from CF_3-terminated thiols having an odd number of carbon atoms (i.e., an "odd−even" or "parity" effect). To rationalize these observations, we proposed that the polar liquids were interacting with terminal dipoles in the CF_3-terminated films; these interactions were enhanced for the SAMs having an even number of carbon atoms due to the orientation of the respective terminal CH_2-CF_3 bonds in the films.

To further probe the relationship(s) between surface dipoles and interfacial wettability, we explore in this paper the structure and wettability of methoxy-terminated SAMs derived from a series of thiols with increasing chain lengths (i.e., $CH_3O(CH_2)_nSH$, where $n = 9-14$). We hypothesized that the introduction of the methoxy terminal group would afford permanent dipoles having orientations distinct from those found in the CF_3-terminated films. We further hypothesized that the presence of the methoxy groups would lead to an increase in the interfacial free energy relative to those of CH_3- and CF_3-terminated SAMs. We chose to prepare and analyze SAMs having relatively long chain lengths because we were concerned that the presence of the terminal methoxy groups might lead to disorder in the films, which could potentially obscure any odd−even dipole effects upon wettability.[34,35] Longer chain lengths offer the potential of enhanced interchain van der Waals interactions that can give rise to stable film structures having a high degree of conformational order.[36,37]

The structures of the methoxy-terminated SAMs reported in this paper were characterized by ellipsometry (to evaluate the thickness of the films) and reflection absorption infrared spectroscopy (to evaluate the orientation and conformational order of the films). The interfacial wettabilities of the SAMs were characterized by contact angle goniometry using a variety of probe liquids classified as polar protic (water, glycerol, formamide, and *N*-methylformamide), polar aprotic (dimethyl formamide, nitrobenzene, acetonitrile, dimethyl sulfoxide), and apolar aprotic (hexadecane).

Experimental Section

Materials. All contacting liquids were of the highest purity available from commercial suppliers and were used without further purification. The starting material 1,10-dibromodecane was purchased from Aldrich Chemical Co.; similarly, the starting ω-bromo alcohols were either purchased from Aldrich or synthesized from commercially available precursors using established methods. The ω-methoxyalkanethiols, $CH_3O(CH_2)_nSH$ ($n = 9-14$), were prepared using the strategy outlined in Scheme 1. For each of the steps, we used synthetic procedures that were analogous for all chain lengths, except for the preparation of 1-bromo-10-methoxydecane. We provide below a detailed description of the preparation of this intermediate; in addition, we provide detailed synthetic procedures for all other steps using $n = 14$ as a representative example. We also provide comprehensive analytical data for all ω-methoxyalkanethiol final products.

Synthesis of 1-Bromo-10-methoxydecane. An aliquot (0.4 mL; 4 mmol) of 1 M NaOMe was added to a solution of 1.1 g (3.7 mmol) of 1,10-dibromodecane dissolved in 50 mL of methanol. The solution was stirred at 70 °C for 12 h, cooled to room temperature, diluted with 10 mL of water, and extracted four times with 20 mL portions of hexanes. The combined organic phases were dried over $MgSO_4$, concentrated under reduced pressure, and purified by column chromatography on silica gel (hexanes/ethyl acetate = 10/1) to afford 0.62 g of 1-bromo-10-methoxydecane in 67% yield. ^{1}H NMR (300 MHz, $CDCl_3$): δ 3.40 (t, $J = 6.9$ Hz, 2 H, CH_2Br), 3.36 (t, $J = 6.6$ Hz, 2 H, CH_2OCH_3), 3.33 (s, 3 H, OCH_3), 1.85 (m, 2 H), 1.54 (m, 2 H), 1.24−1.45 (m, 12 H).

Scheme 1[a]

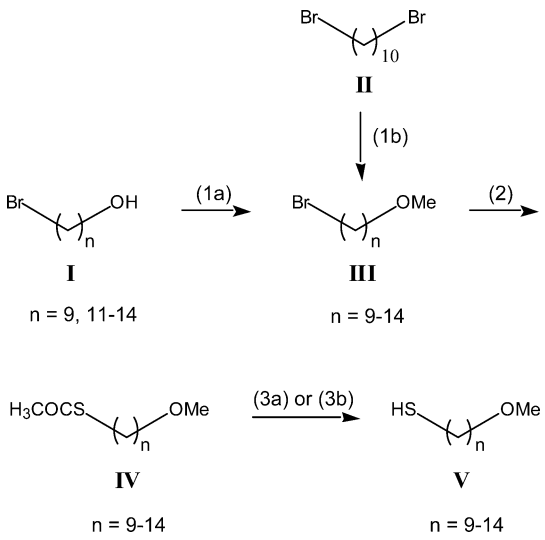

[a] (1a) MeI, NaH, THF; (1b) 1 M NaOMe, MeOH, 70 °C; (2) $KSCOCH_3$, EtOH, reflux; (3a) LAH, THF, then H_2O, 2 M HCl; (3b) H_2SO_4, H_2O, EtOH, 90 °C.

Synthesis of 1-Bromo-14-methoxytetradecane. An aliquot (0.887 g; 3.02 mmol) of 14-bromo-1-tetradecanol was dissolved in 60 mL of THF. To this solution, 1.21 g (30.2 mmol) of NaH (60% dispersion in mineral oil) and 1.9 mL (30 mmol) of MeI were added. After stirring for 4 h at room temperature, the reaction was quenched by adding 50 mL of brine, and the resulting mixture was extracted three times with a 10/1 mixture of hexanes/ethyl acetate. The combined organic phases were dried over $MgSO_4$ and concentrated under reduced pressure to afford crude 1-bromo-14-methoxytetradecane, which was used in the next step without further purification. ^{1}H NMR (300 MHz, $CDCl_3$): δ 3.41 (t, $J = 6.9$ Hz, 2 H, CH_2Br), 3.36 (t, $J = 6.6$ Hz, 2 H, CH_2OCH_3), 3.33 (s, 3 H, OCH_3), 1.85 (m, 2 H), 1.57 (m, 2 H), 1.22−1.43 (m, 20 H).

Synthesis of 14-Methoxytetradecyl Thioacetate. The crude product from the preceding step was dissolved in 70 mL of ethanol. An aliquot (0.690 g; 6.04 mmol) of $KSCOCH_3$ was added, and the mixture was stirred under reflux for 6 h. After cooling to room temperature, 100 mL of water were added, and the aqueous phase was extracted three times with 100 mL portions of a 10/1 mixture of hexanes/ethyl acetate. The combined organic phases were dried over $MgSO_4$ and concentrated under reduced pressure to afford crude 14-methoxytetradecyl thioacetate, which was used in the next step without further purification. ^{1}H NMR (300 MHz, $CDCl_3$): δ 3.36 (t, $J = 6.6$ Hz, 2 H, CH_2OCH_3), 3.33 (s, 3 H, OCH_3), 2.86 (t, $J = 7.3$ Hz, 2 H, $CH_2SCOOCH_3$), 2.32 (s, 3 H, $SCOCH_3$), 1.55 (m, 4 H), 1.20−1.36 (m, 20 H).

Deprotection of the Thioacetates. *Method a: Reduction with LAH*. The crude thioacetate was dissolved in 30 mL of THF, and an aliquot (0.229 g; 6.04 mmol) of LAH was added. The reaction mixture was stirred under reflux for 2 h. After cooling to room temperature, water (~2 mL) was added cautiously, and then the reaction mixture was acidified with 2 M HCl. The solution was diluted with 50 mL of water, and the aqueous phase was extracted three times with 70 mL portions of ethyl acetate. The combined organic phases were washed with saturated aqueous $NaHCO_3$ solution and dried over $MgSO_4$, and the solvent

(34) Miwa, Y.; Machida, K. *J. Am. Chem. Soc.* **1989**, *111*, 7733.
(35) Harder, P.; Grunze, M.; Dahinit, R.; Whitesides, G. M.; Laibinis, P. E. *J. Phys. Chem. B* **1998**, *102*, 426.
(36) Ulman, A.; Eilers, J. E.; Tillman, N. *Langmuir* **1989**, *5*, 1147.
(37) Fenter, P.; Eisenberger, P.; Liang, K. S. *Phys. Rev. Lett.* **1993**, *70*, 2447.

was removed under vacuum. The crude product was purified by column chromatography on silica gel (hexanes/ethyl acetate = 100/1 then 70/1) to afford 14-methoxytetradecanethiol in ~70% yield.

Method b: Acidic Hydrolysis. The crude thioacetate (0.96 g) was dissolved in 130 mL of ethanol, and 36 mL of 5 M sulfuric acid were added. The solution was stirred for 2 h at 90 °C and then cooled to room temperature. The mixture was diluted with 80 mL of water and extracted three times with 130 mL portions of hexanes. The combined organic phases were washed with 100 mL of saturated aqueous $NaHCO_3$ solution and 100 mL of water. The solution was dried with $MgSO_4$ and concentrated under vacuum. Column chromatography of the residue on silica gel afforded 0.55 g (70% yield) of 14-methoxytetradecanethiol.

9-Methoxynonanethiol. ^{1}H NMR (300 MHz, $CDCl_3$): δ 3.36 (t, J = 6.6 Hz, 2 H, CH_2OCH$_3$), 3.33 (s, 3 H, OCH_3), 2.51 (q, J = 7.5 Hz, 2 H, CH_2SH), 1.58 (m, 4 H), 1.26−1.40 (m, 11 H). ^{13}C NMR (75 MHz, $CDCl_3$): δ 72.91, 58.51, 34.01, 29.62, 29.42, 29.40, 28.98, 28.33, 26.09, 24.62. Anal. Calcd for $C_{10}H_{22}OS$: C, 63.10; H, 11.65. Found: C, 63.37; H, 11.48.

10-Methoxydecanethiol. ^{1}H NMR (300 MHz, $CDCl_3$): δ 3.36 (t, J = 6.6 Hz, 2 H, CH_2OCH$_3$), 3.33 (s, 3 H, OCH_3), 2.51 (q, J = 7.5 Hz, 2 H, CH_2SH), 1.57 (m, 4 H), 1.24−1.40 (m, 13 H). ^{13}C NMR (75 MHz, $CDCl_3$): δ 72.94, 58.50, 34.03, 29.63, 29.48, 29.43 (2 C), 29.03, 28.35, 26.11, 24.63. Anal. Calcd for $C_{11}H_{24}OS$: C, 64.64; H, 11.84. Found: C, 64.63; H, 11.65.

11-Methoxyundecanethiol. ^{1}H NMR (300 MHz, $CDCl_3$): δ 3.36 (t, J = 6.6 Hz, 2 H, CH_2OCH$_3$), 3.33 (s, 3 H, OCH_3), 2.51 (q, J = 7.2 Hz, 2 H, CH_2SH), 1.58 (m, 4 H), 1.25−1.41 (m, 15 H). ^{13}C NMR (75 MHz, $CDCl_3$): δ 72.96, 58.52, 34.04, 29.65, 29.54, 29.49 (3 C), 29.06, 28.37, 26.13, 24.65. Anal. Calcd for $C_{12}H_{26}OS$: C, 65.99; H, 12.00. Found: C, 66.02; H, 11.76.

12-Methoxydodecanethiol. ^{1}H NMR (300 MHz, $CDCl_3$): δ 3.33 (t, J = 6.6 Hz, 2 H, CH_2OCH$_3$), 3.30 (s, 3 H, OCH_3), 2.49 (q, J = 7.2 Hz, 2 H, CH_2SH), 1.55 (m, 4 H), 1.22−1.37 (m, 17 H). ^{13}C NMR (75 MHz, $CDCl_3$): δ 72.96, 58.51, 34.04, 29.64, 29.54 (3 C), 29.49 (2 C), 29.05, 28.37, 26.13, 24.64. Anal. Calcd for $C_{13}H_{28}OS$: C, 67.18; H, 12.14. Found: C, 67.02; H, 11.92.

13-Methoxytridecanethiol. ^{1}H NMR (300 MHz, $CDCl_3$): δ 3.33 (t, J = 6.6 Hz, 2 H, CH_2OCH$_3$), 3.30 (s, 3 H, OCH_3), 2.49 (q, J = 7.5 Hz, 2 H, CH_2SH), 1.55 (m, 4 H), 1.20−1.38 (m, 19 H). ^{13}C NMR (75 MHz, $CDCl_3$): δ 72.96, 58.51, 34.04, 29.64, 29.56 (4 C), 29.49 (2 C), 29.06, 28.37, 26.13, 24.64. Anal. Calcd for $C_{14}H_{30}OS$: C, 68.23; H, 12.27. Found: C, 68.25; H, 11.98.

14-Methoxytetradecanethiol. ^{1}H NMR (300 MHz, $CDCl_3$): δ 3.36 (t, J = 6.6 Hz, 2 H, CH_2OCH$_3$), 3.33 (s, 3 H, OCH_3), 2.52 (q, J = 7.5, 2 H, CH_2SH), 1.60 (m, 4 H), 1.22−1.40 (m, 21 H). ^{13}C NMR (75 MHz, $CDCl_3$): δ 72.96, 58.49, 34.04, 29.64, 29.60 (2 C), 29.57 (3 C), 29.49 (2 C), 29.06, 28.36, 26.13, 24.63. Anal. Calcd for $C_{15}H_{32}OS$: C, 69.16; H, 12.38. Found: C, 69.21; H, 12.14.

Substrate Preparation. Gold substrates were prepared under ultrahigh vacuum (UHV) conditions by the evaporation of ~2000 Å of gold onto polished Si(111) wafers, which were precoated with ~100 Å of adhesion-promoting chromium. The resultant gold-coated wafers were rinsed with absolute ethanol and dried with ultrapure nitrogen before SAM formation.

Preparation of SAMs. Ethanolic solutions of the ω-methoxyalkanethiols were prepared at concentrations of ~1 mM in glass vials, which were previously cleaned with piranha solution (3/1 mixture of H_2SO_4/H_2O_2) and rinsed thoroughly with deionized water followed by absolute ethanol. *Caution: piranha solution is highly corrosive, should never be stored, and should be handled with extreme caution*. The evaporated gold substrates were immersed in the thiol solutions for 24 h, rinsed with absolute ethanol, and blown dry using ultrapure nitrogen. The samples were then characterized immediately.

Ellipsometry. A Rudolph Research Auto EL III ellipsometer operating with a He−Ne laser (632.8 nm) at an angle of incidence of 70° from the surface normal was employed to measure the thicknesses of the SAMs. A refractive index of 1.45 was assumed for all of the measurements. The reported values represent the average of at least six measurements taken at different locations on the sample and were reproducible to within ±2 Å.

Polarization Modulation Infrared Reflection Absorption Spectroscopy (PM-IRRAS). A Nicolet MAGNA-IR 860 Fourier transform spectrometer equipped with a liquid nitrogen-cooled mercury−cadmium−telluride (MCT) detector and a Hinds Instruments PEM-90 photoelastic modulator (37 Hz) was employed to obtain the PM-IRRAS data. The spectra were collected at a spectral resolution of 4 cm^{-1} for 64 scans using p-polarized light reflected from the sample at an angle of incidence of 80° from the surface normal.

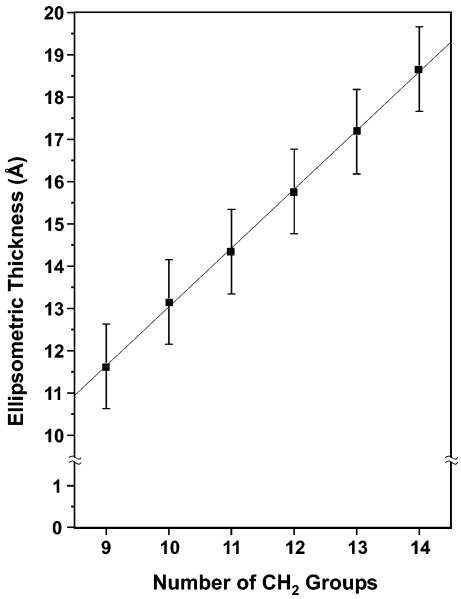

Figure 1. Ellipsometric thicknesses of SAMs on gold derived from $CH_3O(CH_2)_nSH$. The dashed line represents a least-squares fit to the data, where $y = 1.4x - 1.0$. A negative intercept such as that shown here has been observed in plots of ellipsometric thickness for other SAM systems and has been interpreted to reflect the displacement of adventitious material from the surface of gold upon adsorption of the thiols.[18]

Contact Angle Measurements. The contacting liquids, water (H_2O), glycerol (GL), formamide (FA), *N*-methylformamide (MF), *N*,*N*-dimethylformamide (DMF), nitrobenzene (NB), acetonitrile (AC), and hexadecane (HD), were respectively dispensed onto the surfaces of the SAMs using a Matrix Technologies micro-Electrapette 25. Advancing and receding contact angles were measured with a Ramé-Hart model 100 goniometer while keeping the pipet tip in contact with the drop. Each measurement represents the average of both edges of three independent drops of the contacting liquids deposited across the surface of each type of SAM. The observed values were reproducible to within ±1° of those reported.

Results and Discussion

Ellipsometric Thicknesses of the SAMs. Figure 1 summarizes the ellipsometric thicknesses of the SAMs on gold derived from the series of newly prepared ω-methoxyalkanethiols. The data demonstrate that the thicknesses increase from ~11.5 to ~18.5 Å as the number of CH_2 groups increases from 9 to 14, with a slope of ~1.4 Å per methylene group. The observed slope per methylene group and overall thicknesses (equating the contribution from the terminal CH_3O group with that from a terminal CH_3CH_2 group) are indistinguishable from those previously reported for SAMs on gold derived from normal alkanethiols.[18,38−40] The similarity in the data suggests that the incorporation of the ether moiety gives rise to little or no perturbation to the packing and tilt/twist of the SAMs.

(38) Porter, M. D.; Bright, T. B.; Allara, D. L. *J. Am. Chem. Soc.* **1983**, *105*, 4481.
(39) Porter, M. D.; Bright, T. B.; Allara, D. L.; Chidsey, C. E. D. *J. Am. Chem. Soc.* **1987**, *109*, 3559.
(40) Walczak, M. M.; Chung, C.; Stole, S. M.; Widrig, C. A.; Porter, M. D. *J. Am. Chem. Soc.* **1991**, *113*, 2370.

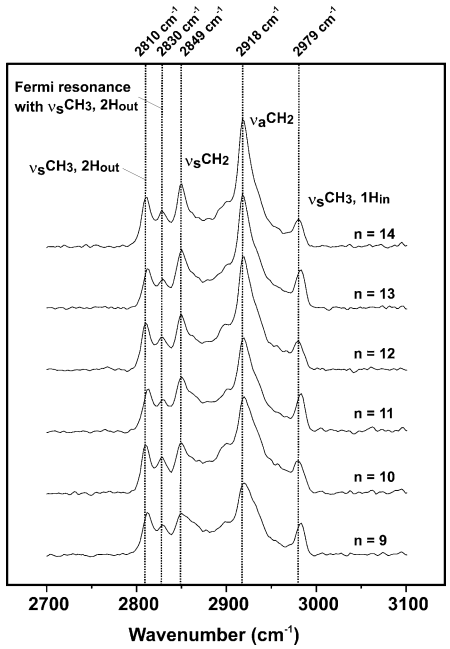

Figure 2. PM-IRRAS spectra of SAMs on gold derived from $CH_3O(CH_2)_nSH$.

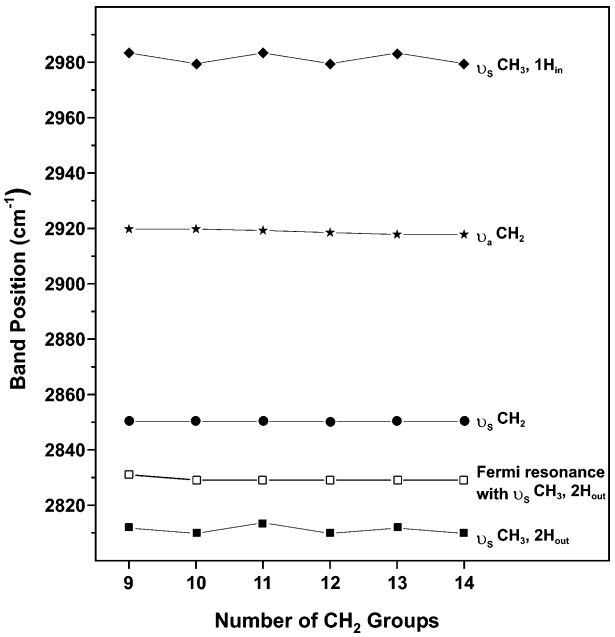

Figure 3. Band positions in the C−H stretching region for SAMs on gold derived from $CH_3O(CH_2)_nSH$ as a function of chain length. The band at ~2930 cm^{-1} arises from a combination of CH_3 deformation modes in Fermi resonance with the A′ stretching mode.[43]

Analysis of the SAMs by Polarization Modulation Infrared Reflection Absorption Spectroscopy (PM-IRRAS). Infrared reflectance spectra of the SAMs on gold derived from the ω-methoxyalkanethiols are shown in Figure 2. A detailed interpretation of the C−H stretching region of SAMs derived from several normal alkanethiols and three related methoxy-terminated thiols has been described elsewhere and provides the basis for our analysis of these spectra.[41−44] Comparison of the data in Figure 2 shows that the intensities of the antisymmetric ($\upsilon_a^{CH_2}$) and symmetric ($\upsilon_s^{CH_2}$) stretching bands increase with increasing chain length, which is consistent with the increasing number of CH_2 groups across the series. Figure 2 also shows that, for all of the SAMs, the $\upsilon_a^{CH_2}$ and $\upsilon_s^{CH_2}$ bands appear at roughly 2919 and 2850 cm^{-1}, respectively, indicating a well-packed and conformationally ordered structure for the methylene chains.[19,39,45]

The spectral data for the $\upsilon_a^{CH_2}$ band positions of the SAMs on gold derived from the ω-methoxyalkanethiols are further highlighted in Figure 3 as a function of chain length. We note that the $\upsilon_a^{CH_2}$ band positions, which are particularly sensitive to the degree of conformational order of the trans-extended methylene backbone,[46] shift from 2919.7 to 2917.8 cm^{-1} as the number of CH_2 groups increases from $n = 9$ to $n = 14$. This small but reproducibly observable shift to smaller wavenumber is consistent with an increase in conformational order with increasing chain length—a phenomenon routinely observed for SAMs on gold derived from normal alkanethiols and attributed to an increase in the interchain van der Waals interactions as the chain length is increased.[39]

Figure 3 also illustrates the band position for the C−H stretching modes of the terminal methoxy group as a function of chain length. A small but significant red shift (~2 cm^{-1}) is observed in both symmetric stretching modes ($\upsilon_s^{CH_3,1H_{(in)}}$ and $\upsilon_s^{CH_3,2H_{(out)}}$) upon switching from odd to even chain lengths. This parity effect is absent in the transmission IR spectra of the corresponding pure thiols (data not shown), suggesting that the monolayer architecture gives rise to the phenomenon. As illustrated in Figure 4, this parity effect can be rationalized on the basis of distinct orientations of the terminal methoxy groups for SAMs composed of odd versus even numbers of methylene groups, which can be inferred from studies of analogous SAMs on gold derived from normal alkanethiols.[19,47] For SAMs having odd numbers of methylenes, we anticipate that the H_3C-O bond will be oriented largely parallel to the surface. Consequently, the H_3C-O dipole will be partially compensated because the negatively charged oxygen of one molecule lies near the positively charged methyl carbon of an adjacent molecule. This interaction can plausibly increase the H_3C-O bond length and lower the C−O stretching frequency.[48] In contrast, the H_3C-O bond in SAMs containing even numbers of methylenes will point more toward the surface normal, leaving the H_3C-O dipole largely uncompensated and the H_3C-O stretching frequency unaffected. Unfortunately, we failed to monitor the C−O spectral region in our analyses; nevertheless, because the two symmetric C−H stretching modes of the methyl group are coupled to the stretching mode of the H_3C-O bond, we can evaluate this effect indirectly.[49] In particular, our model would predict lower methyl C−H stretching frequencies for SAMs composed of even numbers of methylenes when compared to those of SAMs composed of odd numbers of methylenes, which is consistent with our observations (see Figures 2 and 3).

A further examination of Figure 2 reveals that the *intensities* of the methyl C−H stretching bands are also

(41) Bellamy, L. J. *The Infrared Spectra of Complex Molecules*; Chapman & Hall: London, 1980.
(42) Nuzzo, R. G.; Korenic, E. M.; Dubois, L. H. *J. Chem. Phys.* **1990**, *93*, 767.
(43) Ong, T. H.; Davies, P. B.; Bain, C. D. *Langmuir* **1993**, *9*, 1836.
(44) Laibinis, P. E.; Bain, C. D.; Nuzzo, R. G.; Whitesides, G. M. *J. Phys. Chem.* **1995**, *99*, 7663.
(45) MacPhail, R. A.; Strauss, H. L.; Snyder, R. G.; Elliger, C. A. *J. Phys. Chem.* **1982**, *88*, 334.
(46) Shon, Y.-S.; Lee, S.; Colorado, R., Jr.; Perry, S. S.; Lee, T. R. *J. Am. Chem. Soc.* **2000**, *122*, 7556.
(47) Tao, Y.-T. *J. Am. Chem. Soc.* **1993**, *115*, 4350.
(48) Bellamy, L. J.; Williams, R. L. *J. Chem. Soc.* **1957**, 4294.
(49) Colthup, N. B.; Daly, L. H.; Wiberley, S. E. *Introduction to Raman and Infrared Spectroscopy*, 3rd ed.; Academic Press: San Diego, CA, 1982.

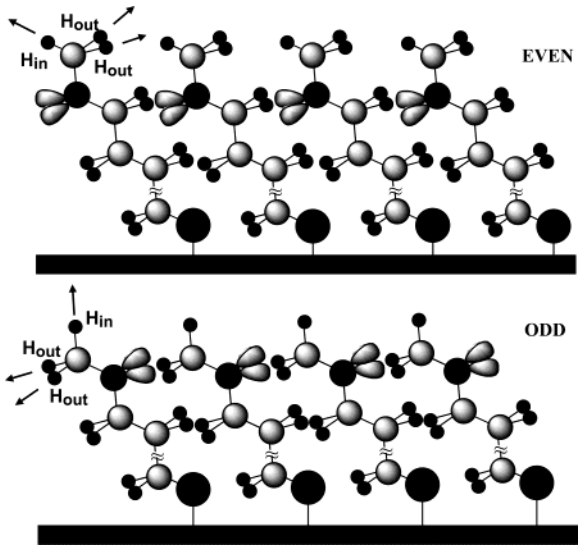

Figure 4. Proposed molecular orientations and symmetric C−H stretching modes of the methoxy group for SAMs on gold derived from $CH_3O(CH_2)_nSH$ as a function of odd vs even chain lengths. These structures serve only to illustrate the relative alternation of the terminal group orientation as a function of chain length and are drawn by analogy to SAMs on gold derived from normal alkanethiols.[19,47]

affected by the parity of the hydrocarbon backbone. The intensity of the first C−H symmetric stretching mode ($\upsilon_s^{CH_3,1H_{(in)}}$) at 2980 cm^{-1} alternates between odd and even chain lengths and is greater for odd-numbered methylene chains. The intensity of the second C−H symmetric stretching mode ($\upsilon_s^{CH_3,2H_{(out)}}$) at 2810 cm^{-1} alternates in the opposite sense. On the basis of our structural model (see Figure 4), the terminal $CH_{(in)}$ bond in SAMs having odd numbers of methylenes lies roughly normal to the surface; in contrast, for SAMs having even numbers of methylenes, this bond lies more parallel to the surface. Consequently, the intensity of the $CH_3,1H_{(in)}$ mode should be enhanced for SAMs having odd numbers of methylenes, which is consistent with our observations. Our model also predicts that the $CH_3,2H_{(out)}$ modes will be diminished for SAMs having odd numbers of methylenes because the corresponding C−H bonds likely point along the surface parallel. Again, this model is consistent with our experimental observations. Despite the discussion presented here, we wish to emphasize that any inferences derived from intensity data are merely qualitative for two reasons: (1) a quantitative comparison between spectra of various samples requires remarkably precise control of the experimental conditions,[19,47] and (2) the alternative approach involving the use of ratios of peaks within a spectrum followed by comparison is not possible here due to insufficient resolution of the peaks of interest.

Contact Angle Measurements. We examined the advancing and receding contact angles of a variety of probe liquids on the surfaces of the methoxy-terminated SAMs. Figure 5 displays the advancing contact angles (θ_a) of glycerol (GL), formamide (FA), water (H_2O), dimethyl sulfoxide (DMSO), *N*-methylformamide (MF), nitrobenzene (NB), *N*,*N*-dimethylformamide (DMF), hexadecane (HD), and acetonitrile (AC) on these SAMs. The previously measured wettability data for GL, FA, H_2O, and HD on SAMs on gold derived from the lone adsorbate $CH_3O(CH_2)_{11}SH$ are generally comparable to those observed here.[18,44,50] Moreover, for all test liquids examined, we have found that the methoxy-terminated SAMs are more

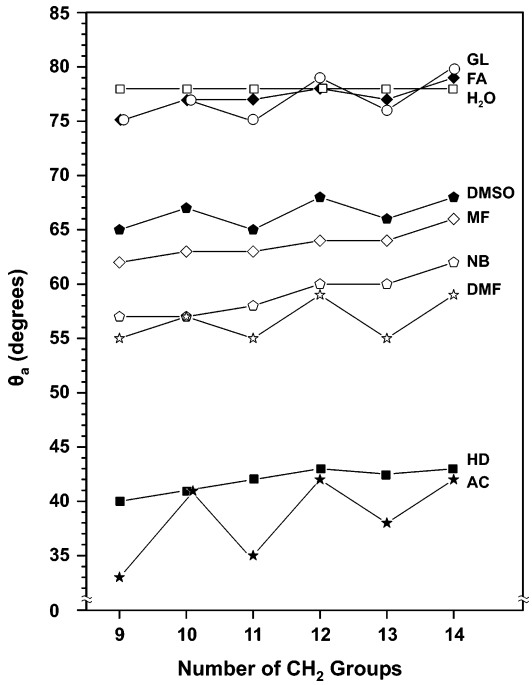

Figure 5. Advancing contact angles (θ_a) as a function of chain length for various liquids on the surfaces of SAMs on gold derived from $CH_3O(CH_2)_nSH$: ○, glycerol (GL); ◆, formamide (FA); □, water (H_2O); ⬟, dimethyl sulfoxide (DMSO); ◇, methylformamide (MF); ⬠, nitrobenzene (NB); ☆, dimethylformamide (DMF); ■, hexadecane (HD); ★, acetonitrile (AC).

wettable than SAMs derived from normal alkanethiols having analogous chain lengths (i.e., $CH_3(CH_2)_{n+1}SH$). The enhanced wettability of the methoxy-terminated SAMs arises from the exposure of the polar CH_3O groups at the interface, which raises the surface free energy.[18]

For all probe liquids except water, the advancing contact angles were observed to increase with increasing chain length across the series of methoxy-terminated SAMs. This phenomenon can be viewed mentally by drawing a best-fitting line through the contact angle data in Figure 5 for any individual probe liquid as a function of chain length; this exercise yields a positive slope in all cases excluding water. The enhanced wettability of the SAMs having the shortest chain lengths probably arises from one or both of the following effects: (1) the probe liquids might be sensing attractive van der Waals interactions from the underlying gold substrate, which would be stronger for the SAMs having shorter chain lengths,[51] and/or (2) the probe liquids might be interacting with exposed oxygen atoms and methylene groups, which are likely to be more prevalent in SAMs having short chain lengths because of their enhanced disorder (a feature consistent with the PM-IRRAS data described above).[39,46]

Many of the probe liquids also exhibited parity effects (i.e., systematic variations in wettability as a function of the odd- versus even-numbered chain length of the methoxy-terminated SAMs). In particular, GL, DMSO, DMF, and AC showed reproducible parity effects, with lower contact angles for n = odd and higher contact angles

(50) Compared to the data in ref 18 for this SAM, our values for the contact angles of water and HD are higher by 4° and 7°, respectively. However, compared to the data in ref 44 for this SAM, our values for the contact angle of FA are indistinguishable (±1°), while those of GL and water are lower by ~7°, and those of HD are higher by 5°. Although we are unable to rationalize the indicated discrepancies, we note that our data were found to be reproducible by multiple independent researchers using multiple independently prepared samples.

(51) Miller, W. J.; Abbott, N. L. *Langmuir* **1997**, *13*, 7106.

Table 1. Receding Contact Angles and Hysteresis ($\Delta\theta$) for SAMs on Gold Derived from $CH_3O(CH_2)_nSH$[a]

	receding contact angles, θ_r (hysteresis, $\Delta\theta = \theta_a - \theta_r$)								
$CH_3O(CH_2)_nSH$	*W*	GL	FA	DMSO	MF	DMF	NB	HD	AC
$n = 9$	68 (10)	65 (10)	64 (11)	56 (9)	52 (10)	43 (12)	44 (13)	26 (14)	17 (16)
$n = 10$	68 (10)	68 (9)	66 (11)	58 (9)	54 (9)	45 (12)	45 (12)	29 (12)	29 (12)
$n = 11$	68 (10)	67 (8)	66 (11)	56 (9)	52 (11)	53 (12)	45 (13)	31 (11)	25 (10)
$n = 12$	68 (10)	71 (8)	68 (10)	61 (7)	55 (9)	48 (11)	46 (14)	32 (11)	32 (10)
$n = 13$	70 (9)	68 (8)	67 (10)	60 (6)	55 (9)	44 (11)	47 (13)	33 (10)	30 (8)
$n = 14$	71 (7)	72 (8)	69 (10)	62 (6)	57 (9)	48 (11)	49 (13)	35 (8)	34 (8)

[a] All values are reported in degrees.

for n = even. For certain other liquids (e.g., FA, MF, and NB), the systematic nature of this variation was partially obscured by the concurrent increase in contact angle with increasing chain length described in the preceding paragraph. The advancing contact angles of MF, for example, were observed to increase from $n = 9$ (62°) to $n = 14$ (66°), with modest increases occurring when the number of methylenes was varied from n = odd to n = even but negligible increases occurring when the number of methylenes was varied from n = even to n = odd. Unfortunately, our contact angle measurements were insufficiently precise (±1°) to claim the parity effect for HD with any degree of certainty. Water exhibited a markedly distinct behavior, being completely insensitive to any variations in chain length. We attribute this invariance to the small size of the water molecule, which enables it to intercalate into the monolayer and disorder the outer layer of atoms during the contact angle measurement.[52]

The observed parity effects in the contact angle data are undoubtedly due to the systematically varying orientation of the terminal methoxy group in the SAMs having odd-numbered versus even-numbered methylene chains (see Figure 4). In cases where n = odd, the terminal H_3C-O bond points away from the surface normal, exposing the underlying polar oxygen atom and thus enhancing the attractive interactions between the contacting liquids and the film relative to the cases where n = even.

The measured receding contact angles (θ_r) and the calculated values of contact angle hysteresis ($\Delta\theta = \theta_a - \theta_r$) are listed in Table 1. Given that the receding contact angles follow the general patterns of the advancing contact angles, we offer here no detailed analysis of these data. Values of contact angle hysteresis, however, allow us to evaluate the heterogeneity and/or roughness of the surfaces of the SAMs.[53−55] These values are comparable with those reported for SAMs on gold derived from normal alkanethiols,[56] suggesting that the surfaces of the methoxy-terminated SAMs are homogeneous and macroscopically smooth over all of the chain lengths examined. In addition, the data in Table 1 show that the values of hysteresis decrease as the length of the methylene chain increases, regardless of the probe liquid employed. This observation is consistent with our PM-IRRAS data (vide supra), which indicate increasing conformational order with increasing chain length for these SAMs.

Works of Adhesion. To probe the physical origins of the wettabilities of the methoxy-terminated SAMs, we calculated the work of adhesion (W_{SL}) between the various probe liquids and the surfaces of the SAMs using the modified Good−Girifalco−Fowkes relation (eq 1) , which

$$W_{SL} = W_{SL}^{\,d} + W_{SL}^{\,p} \qquad (1)$$

separates the contributions to the total work of adhesion (W_{SL}) into dispersive (W_{SL}^{d}) and polar (W_{SL}^{p}) components.[57−60] In this approach, the works of adhesion are calculated in the following manner: $W_{SL} = \gamma_L(1 + \cos\theta_a)$, $W_{SL}^{d} = 2(\gamma_S^{d}\gamma_L^{d})^{1/2}$, and $W_{SL}^{p} = W_{SL} - W_{SL}^{d}$. The value of γ_S^{d} can be estimated for each surface by using hexadecane as the probe liquid and assuming that $W_{SL} = W_{SL}^{d}$ (i.e., $\gamma_L(1 + \cos\theta_a) = 2(\gamma_S^{d}\gamma_L^{d})^{1/2}$ and $\gamma_L = \gamma_L^{d} = 27.5$ mJ·m^{-2}).[61,62] Similarly, the value of γ_L^{d} can be estimated for each probe liquid by using SAMs derived from normal alkanethiols (i.e., $CH_3(CH_2)_nSH$, where $n = 12-15$) as models of purely dispersive surfaces, and again assuming that $W_{SL} = W_{SL}^{d}$.[58] The values of γ_L^{d} obtained using this approach are provided in Table 2 along with literature values of γ_L.[63]

Table 2. Values of Surface Tension (mJ·m^{-2}) for the Various Contacting Liquids and the Methoxy-Terminated SAMs[61−63]

contacting liquid	γ_L (mJ·m^{-2})	γ_L^{d} (mJ·m^{-2}) ($\pm\Delta\gamma_L^{d}$)
water (W)	72.4	23.8 (±1.4)
glycerol (GL)	63.4	32.6 (±1.5)
formamide (FA)	58.0	33.5 (±1.4)
nitrobenzene (NB)	43.8	42.7 (±1.2)
dimethyl sulfoxide (DMSO)	43.5	33.3 (±1.0)
methylformamide (MF)	38.8	27.5 (±0.8)
dimethylformamide (DMF)	36.8	30.0 (±0.8)
hexadecane (HD)	27.5	27.5 (±0.5)
acetonitrile (AC)	27.0	19.3 (±0.5)

Figures 6−8 show the various works of adhesion (W_{SL}, W_{SL}^{d}, and W_{SL}^{p}, respectively) as a function of chain length for the methoxy-terminated SAMs. For all probe liquids (excluding water), the total and component works of adhesion were observed to decrease with increasing chain length. The decreasing trend for W_{SL}^{d} (Figure 7) can be rationalized on the basis of the effects described above (i.e., due either to a progressive decrease in the attractive van der Waals interactions from the underlying gold substrate[51] and/or a progressive loss of liquid−solid molecular interactions concomitant with an increase in conformational order of the interface).[46,64] Similarly, the average decreasing trend for W_{SL}^{p} (Figure 8) might be

(52) Bain, C. D.; Whitesides, G. M. *J. Am. Chem. Soc.* **1988**, *110*, 5897.
(53) Eick, J. D.; Neumann, A. W. *J. Colloid Interface Sci.* **1975**, *53*, 235.
(54) Wu, S. *Polymer Interface and Adhesion*; Marcel Dekker: New York, 1982.
(55) Joanny, J. F.; de Gennes, P. G. *J. Chem. Phys.* **1984**, *87*, 552.
(56) Laibinis, P. E.; Whitesides, G. M.; Allara, D. L.; Tao, Y.-T.; Parikh, A. N.; Nuzzo, R. G. *J. Am. Chem. Soc.* **1991**, *113*, 7152.
(57) Good, R. J.; Girifalco, L. A. *J. Phys. Chem.* **1960**, *64*, 561.
(58) Fowkes, F. M. *J. Phys. Chem.* **1963**, *67*, 2538.
(59) Dann, J. R. *J. Colloid Interface Sci.* **1970**, *32*, 302.
(60) Dann, J. R. *J. Colloid Interface Sci.* **1970**, *32*, 321.
(61) Colorado, R., Jr.; Lee, T. R. *J. Phys. Org. Chem.* **2000**, *13*, 796.
(62) Colorado, R., Jr.; Lee, T. R. *Langmuir* **2003**, *19*, 3288.
(63) Fowkes, F. M.; Riddle, F. L., Jr.; Pastore, W. E.; Weber, A. A. *Colloid Surf.* **1990**, *43*, 367.
(64) We note that the data for W_{SL}^{d} (Figure 7) and the contact angles of hexadecane (Figure 5) appear to become constant for $n \geq 12$, which suggests that the dispersive interactions become constant for the longer chain lengths. This observation, however, does not permit us to distinguish between the two proposed mechanisms, given that the gold−liquid van der Waals interactions likely become imperceptibly weak at the longer distances and/or the interfacial order likely becomes indistinguishably crystalline for the longer chain lengths.

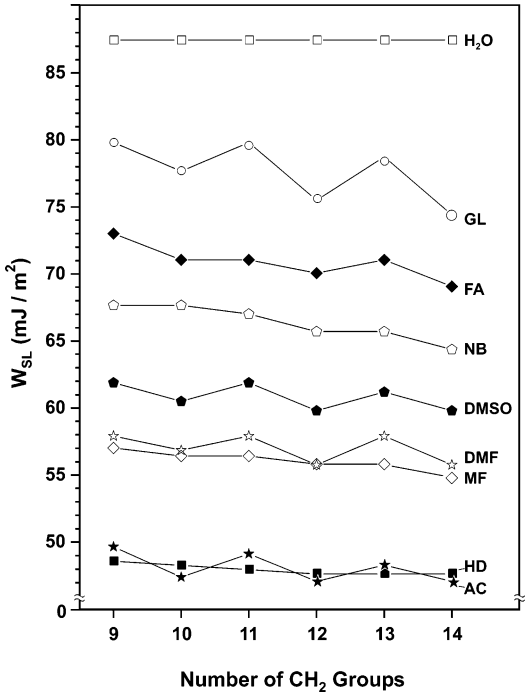

Figure 6. Work of adhesion W_{SL} of SAMs on gold derived from $CH_3O(CH_2)_nSH$ as a function of chain length: □, water (H_2O); ○, glycerol (GL); ◆, formamide (FA); ⬠, nitrobenzene (NB); ⬟, dimethyl sulfoxide (DMSO); ☆, dimethylformamide (DMF); ◇, methylformamide (MF); ■, hexadecane (HD); ★, acetonitrile (AC).

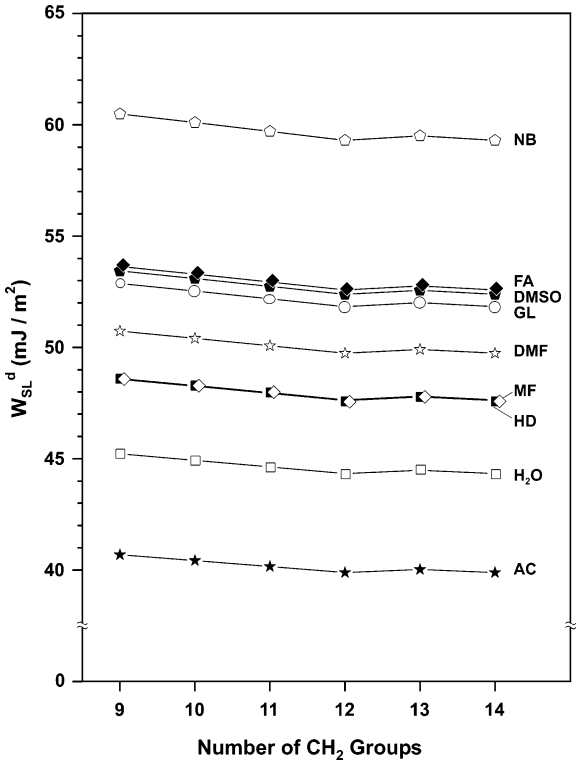

Figure 7. Dispersive component of the work of adhesion W_{SL}^d of SAMs on gold derived from $CH_3O(CH_2)_nSH$ as a function of chain length: ⬠, nitrobenzene (NB); ◆, formamide (FA); ⬟, dimethyl sulfoxide (DMSO); ○, glycerol (GL); ☆, dimethylformamide (DMF); ◇, methylformamide (MF); ■, hexadecane (HD); □, water (H_2O); ★, acetonitrile (AC).

related to a decrease in intercalation of the probe liquids as the interface becomes more highly ordered, which can plausibly lead to a decrease in attractive dipole−dipole

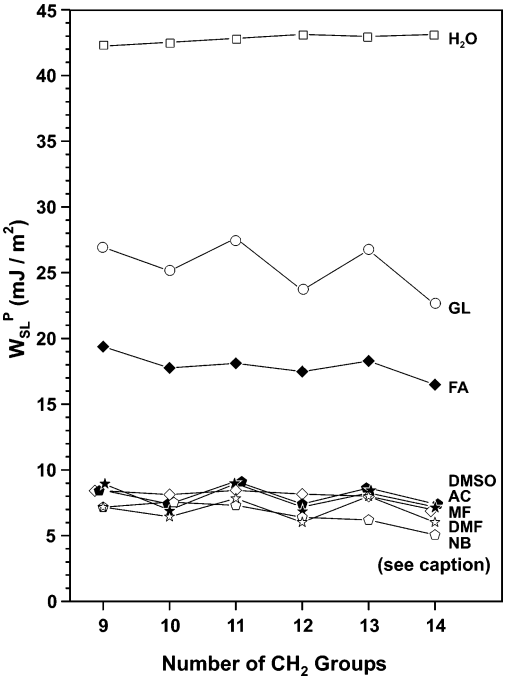

Figure 8. Polar component of the work of adhesion W_{SL}^p of SAMs on gold derived from $CH_3O(CH_2)_nSH$ as a function of chain length: □, water (H_2O); ○, glycerol (GL); ◆, formamide (FA); ⬟, dimethyl sulfoxide (DMSO); ★, acetonitrile (AC); ◇, methylformamide (MF); ☆, dimethylformamide (DMF); ⬠, nitrobenzene (NB).

Table 3. Experimental Uncertainty ($\pm$mJ·m^{-2}) in the Values Obtained for the Works of Adhesion

	maximum uncertainty ($\pm$mJ·m^{-2})								
	W	GL	FA	DMSO	MF	DMF	NB	HD	ACN
W_{SL}	1.2	1.1	1.0	0.7	0.6	0.5	0.7	0.3	0.3
W_{SL}^d	1.9	1.9	1.8	1.5	1.4	1.4	1.6	0.7	1.0
W_{SL}^p	3.1	3.0	2.8	2.2	2.0	1.9	2.3	1.0	1.3

[a] The uncertainties were calculated using standard error propagation methods based on the equations in the text describing the various works of adhesion. The estimated error in the contact angle values is $\pm$1°.

and/or H-bonding interactions (with the latter being relevant only when polar protic liquids are involved).

Further analysis of Figure 8 reveals the presence of small parity effects (i.e., slightly higher values of W_{SL}^p for n = odd and slightly lower values for n = even) for all of the probe liquids (excluding water). While the magnitudes of the variations are arguably insubstantial given the magnitude of the experimental error (see Table 3), their systematic and reproducible nature is striking. It is important to note that this effect appears to be manifested in W_{SL}^p rather than W_{SL}^d (see Figure 7), which argues for a surface dipole origin.[65] As noted above, the terminal group orientation for n = odd (Figure 4) will likely lead to the exposure of underlying polar oxygen atoms, which can enhance the attractive interactions with polar contacting liquids and thus lead to greater values of W_{SL}^p relative to that for n = even. Moreover, for the two liquids with the most pronounced odd−even variation in W_{SL}^p (i.e., GL and AC), the amplitude appears to increase with increasing chain length, which is consistent with a model in which the surface dipoles in both odd- and even-

(65) We attribute these small parity effects to surface dipoles rather than H-bonding, due to the fact that the phenomenon is apparent with certain liquids having no obvious ability to H-bond with surface methoxy groups (e.g., AC and DMF).

numbered chain length molecules reach more highly fixed orientations as the conformational order of the films increases.

Conclusions

The exposure of polycrystalline gold surfaces to solutions containing ω-methoxyalkanethiols ($CH_3O(CH_2)_nSH$) having varied chain lengths ($n = 9-14$) led to the formation of highly oriented SAMs in which the conformational order and the contact angles of the films were observed to increase with increasing chain length. Analysis by PM-IRRAS revealed a systematic variation in both the frequency and the intensity of the C−H symmetric stretching bands of the methoxy group as a function of odd-numbered versus even-numbered methylene groups in the adsorbate. This variation was attributed to alternating structural changes in the terminal portion of the films, which were correlated with systematic odd versus even variations in the wettabilities of polar contacting liquids on these SAMs. On the basis of the contact angle measurements, corresponding works of adhesion were calculated, which revealed the influence of surface dipole effects upon the wettabilities.

Acknowledgment. The National Science Foundation (DMR-9700662), the Robert A. Welch Foundation (Grant No. E−1320), and the Texas Advanced Research Program (003652-0307-2001) provided generous support for this research. We thank our colleagues Steve Baldelli and Roman Czernuszewicz for their insight and helpful comments regarding the IR analyses. I.W. gratefully acknowledges support from the "Fonds zur Foerderung der wissenschaftlichen Forschung" (FWF) in the form of an "Erwin-Schroedinger" Postdoctoral Fellowship (J1804-CHE).

LA035227X